

Remote-plasma chemical vapor deposition of conformal ZrB_2 films at low temperature: A promising diffusion barrier for ultralarge scale integrated electronics

Junghwan Sung

Department of Materials Science and Engineering, University of Illinois at Urbana-Champaign, Illinois 61801 and Fredrick Seitz Materials Research Laboratory, University of Illinois at Urbana-Champaign, Illinois 61801

Dean M. Goedde and Gregory S. Girolami

Department of Chemistry, University of Illinois at Urbana-Champaign, Illinois 61801 and Fredrick Seitz Materials Research Laboratory, University of Illinois at Urbana-Champaign, Illinois 61801

John R. Abelson^{a)}

Department of Materials Science and Engineering, University of Illinois at Urbana-Champaign, Illinois 61801 and Fredrick Seitz Materials Research Laboratory, University of Illinois at Urbana-Champaign, Illinois 61801

(Received 17 August 2001; accepted for publication 20 November 2001)

High-quality ZrB_2 thin films have been deposited at substrate temperatures as low as 300°C by a new method: remote hydrogen-plasma chemical vapor deposition from the single-source precursor $\text{Zr}(\text{BH}_4)_4$. Carrying out the deposition in the presence of atomic hydrogen generates films with properties that are far superior to those deposited by purely thermal methods; the latter are boron-rich, oxidize readily in air, and adhere poorly to the substrates. In contrast, the films generated at a substrate temperature of 300°C in the presence of atomic H have a B/Zr ratio of 2, a resistivity of $40\ \mu\Omega\ \text{cm}$, an oxygen content of $\leq 4\ \text{at.}\%$, and are fully conformal in deep vias. A 20 nm thick amorphous film of ZrB_2 on *c*-Si(001) prevents Cu indiffusion after 30 min at 750°C . We propose that the beneficial effects of atomic hydrogen can be attributed to promoting the desorption of diborane from the growth surface. © 2002 American Institute of Physics.

[DOI: 10.1063/1.1436296]

I. INTRODUCTION

There is considerable current interest in the development of new and improved materials to serve as diffusion barriers for copper, owing to the fact that copper is rapidly becoming the metal of choice for interconnects in ultralarge scale integrated circuits (ULSI).^{1,2} In the absence of a diffusion barrier, copper and silicon rapidly combine to form copper silicide phases, which destroy device performance owing to their high electrical resistivities. One of the most difficult challenges in integrated circuit fabrication is to line high-aspect vias with a thin coating of a diffusion barrier before the vias are filled with metal. As device feature sizes shrink below $0.12\ \mu\text{m}$, conventional physical vapor deposition (PVD) methods become incapable of providing good step coverage, even with modifications such as ion-enhanced forward recoil of deposited atoms. In addition, as the diffusion barrier becomes thinner, amorphous materials become increasingly preferable because the absence of grain boundaries reduces the diffusivity of foreign atoms.³ Thus the development of new processes to deposit conformal, amorphous barriers with low resistivities is one of the most important challenges for the next generation of ULSI.

The group IV transition metal diborides TiB_2 , ZrB_2 , and HfB_2 are particularly interesting as copper diffusion barriers

because they are thermodynamically stable in contact with Cu, Si, and SiO_x and their bulk resistivities are remarkably low ($\sim 10\ \mu\Omega\ \text{cm}$). In this work we demonstrate the growth of thin ZrB_2 films with resistivities below $60\ \mu\Omega\ \text{cm}$. These films are amorphous and remain amorphous during annealing up to 700°C . In contrast, transition metal nitrides (such as TiN , TaN , and WN_x) crystallize easily, and the resulting grain boundaries enable fast Cu diffusion. Amorphous films of ternary materials (W–Si–N, Ti–Si–N, etc.) are less prone to crystallize but suffer from high resistivities of $> 300\ \mu\Omega\ \text{cm}$.^{4–6}

Chemical vapor deposition (CVD) and PVD methods to deposit films of group 4 transition metal diborides have been previously described.^{7–10} In conventional CVD of ZrB_2 films, the precursors ZrCl_4 and BCl_3 are reduced with H_2 . This approach yields high-quality films but requires a substrate temperature above 600°C , which is far too high for ULSI processing.¹¹ At lower temperatures, overstoichiometric films with B/Zr atomic ratios greater than 2 are typically observed. This is a general phenomenon: excess B is observed in films grown by other CVD and PVD methods if the substrate temperature is below 600°C .^{12,13} ZrB_2 does not have a wide phase field: the B/Zr ratio ranges only from 1.94 to 2.03 at room temperature.¹⁴ Therefore a significantly overstoichiometric film must consist of a mixture of ZrB_2 and B. Thermodynamic studies show that, in the $\text{ZrCl}_4\text{--BCl}_3\text{--H}_2$

^{a)}Electronic mail: abelson@uiuc.edu

system, the mixed phase is favored at low temperatures and high supply rates of BCl_3 .¹⁵ To obtain high conductivity and mechanical hardness, transition metal diborides must be nearly stoichiometric; excess boron degrades the properties.^{16,17} Controlling the film composition is thus a critical issue.

An attractive, and single-source, CVD precursor for ZrB_2 has been described: tetrakis(tetrahydroborato)zirconium(IV), $\text{Zr}(\text{BH}_4)_4$, hereafter referred to as zirconium borohydride.¹⁸ This compound has the highest vapor pressure of any known zirconium compound (~ 1 Torr at 0°C),¹⁹ contains no undesirable impurities such as carbon, oxygen, or chlorine, and decomposes to produce conductive films at substrate temperatures as low as 180°C .²⁰ In principle, zirconium borohydride should transform to stoichiometric ZrB_2 by means of the overall reaction:



Although the formation of diborane and molecular hydrogen during CVD has been confirmed by gas chromatography,^{18,20} in fact the films obtained by thermal CVD have B/Zr ratios greater than 2:1. Evidently, the formation and desorption of B_2H_6 molecules is inefficient relative to desorption of H_2 . The excess boron becomes trapped inside the films, causing the latter to have high electrical resistivities and to oxidize readily in air.

In this work we show that the excess boron can be removed from the growth surface by directing a flux of atomic hydrogen, generated by a remote microwave plasma discharge of H_2 , onto the substrate during the CVD process; this technique is referred to as remote-plasma CVD (RPCVD). The atomic hydrogen enhances the formation and desorption of diborane at substrate temperatures below 300°C . This approach produces stoichiometric, amorphous ZrB_2 films with low resistivities ($40\text{--}60 \mu\Omega\text{ cm}$). We show that the films can be deposited conformally, and that they are excellent diffusion barriers for Cu. The growth kinetics and the resulting film properties will also be described.

II. EXPERIMENTAL SECTION

In order to minimize carbon and oxygen contamination, zirconium borohydride was prepared by a solvent-free method from ZrCl_4 and LiBH_4 .²¹ Glass (Corning 7059), and *n*- and *p*-type Si(100) substrates were prepared by standard RCA cleaning to remove organic and metallic residues. For Si substrates, the RCA cleaning was followed by a dip in 10% HF to remove surface oxide.

The deposition chamber (Fig. 1) had a base pressure of 1×10^{-7} Torr. The $\text{Zr}(\text{BH}_4)_4$ reservoir was maintained at 0°C in an ice bath and the precursor pressure in the chamber was maintained between 1.0×10^{-5} and 0.8×10^{-3} Torr by adjusting the precursor flow rate with a needle valve. The chamber was equipped with a mass spectrometer, which was used to determine the relative partial pressures of the precursor and stable reaction by-products.

The precursor was delivered to the reaction surface through a 2.5 cm i.d. reaction tube that terminated just above the substrate. The spacing between the end of the tube and

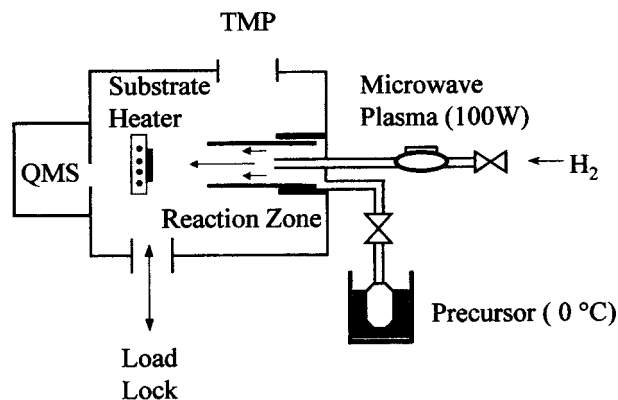


FIG. 1. Diagram of apparatus used for remote hydrogen-plasma chemical vapor deposition.

the surface was ~ 3 cm but could be varied in order to change the gas conductance, and thus the relationship between precursor flow rate and deposition pressure. Atomic hydrogen was generated in a 0.625 cm o.d. Pyrex tube by plasma dissociation of molecular H_2 with a 100 W microwave power source (Ophos MPG-4M). Throughout our experiment, the partial pressures of zirconium borohydride and H_2 were kept below 10^{-4} and 3×10^{-3} Torr, respectively. Under these conditions, the mean free paths (~ 5 cm) of both species are larger than the length of the mixing zone (3 cm) inside the chamber. The absolute flux of atomic H at the substrate is difficult to estimate because the dissociation fraction in the excitation zone and the rate of recombination of atomic hydrogen to molecular hydrogen on the wall of the Pyrex tube are not known.

The sheet resistance of the deposited ZrB_2 films was measured using the four-point probe technique. Film thicknesses were measured by stylus profilometry and by scanning electron microscopy (SEM). The average growth rate was calculated by dividing the film thickness by deposition time. Film composition was measured by Rutherford backscattering spectrometry (RBS) with 2 MeV He^+ . Secondary ion mass spectra (SIMS) were measured with a Cameca IMS 5f instrument, and x-ray photoelectron spectra (XPS) were measured with a PHI 5400 spectrometer. X-ray diffraction (XRD) profiles were obtained on a Rigaku D-MAX diffractometer.

To analyze the surface reactions of zirconium borohydride, *in situ* Fourier transform infrared spectroscopy (FTIR) in reflectance mode was used in a different vacuum system. To observe the initial stage of reactions, a multilayer dielectric stack was used for the substrate. This substrate consisted of a double polished Si wafer with a thermal oxide thickness of 1040 nm on both sides and an Al backside coating; we previously showed that a combination of coherent and incoherent multiple internal reflections greatly enhances the IR sensitivity.²²

For diffusion experiments, PVD copper was deposited on top of a RPCVD ZrB_2 film. A multilayer structure consisting of $\text{Cu}(100 \text{ nm})/\text{ZrB}_2(20 \text{ nm})/\text{Si}(100)$ was annealed in a tube furnace at $500\text{--}800^\circ\text{C}$ for 30 min in flowing N_2 . The Cu depth profile was measured by RBS after annealing.

The RBS data were fitted using the RUMP software package.²³ After the annealed multilayers were characterized, the Cu and ZrB₂ films were etched away with a 20% HNO₃–10% HCl solution, and then atomic force microscopy (AFM) and scanning electron microscopy (SEM) were used to examine the morphology of the exposed Si surface.

For the step coverage experiments, 0.3 μm diameter vias with an aspect ratio of 5:1 were fabricated by reactive ion etching of a 1.5 μm thick SiO₂ layer on Si(100). After ZrB₂ deposition, the substrate was cleaved, etched with a 1% HF solution to accentuate the ZrB₂/SiO₂ interface, and coated with 0.5 nm of gold. The step coverage was determined by SEM.

III. RESULTS AND DISCUSSION

A. Thermal CVD

For comparison with the studies described below, we briefly summarize the properties of films grown by thermal CVD from Zr(BH₄)₄. As mentioned in the Introduction, thermal CVD of Zr(BH₄)₄ at substrate temperatures of 250–450 °C affords boron-rich films with B/Zr ratios near 3. The thermally deposited “ZrB_{2+x}” films prepared under these conditions often are blistered.²⁰ The blistering, which is present even before the films are removed from the deposition chamber and handled in air, is most severe when the growth rate is relatively high (>100 nm/min) and the temperature is relatively low (<450 °C). These observations indicate that the blistering occurs during deposition and is caused by the formation of gas inside the films, possibly due to the slow release of diborane, rather than by thermal stress during heating/cooling steps or by air oxidation after the films are removed from the growth chamber.

Films of ZrB_{2+x} deposited at substrate temperatures below 450 °C and at lower growth rates generally do not blister, but tend to oxidize readily. These films exhibit XRD peaks that correspond to boric acid B(OH)₃, but none due to B₂O₃ or ZrO₂. When boric acid starts to form, the films begin to peel from their substrates. The ease with which the thermally deposited ZrB_{2+x} films oxidize in air suggests that the excess boron is present not as elemental boron, which is relatively slow to oxidize at room temperature, but rather in the form of BH_x fragments.

If BH_x fragments are present in the thermally deposited ZrB_{2+x} films, they should give characteristic IR bands. Figure 2 shows the IR reflectance spectrum obtained from a SiO₂ surface after it had been heated to 250 °C and exposed to 1×10^{-6} Torr of Zr(BH₄)₄ for 67 s. Two broad absorption bands, at 2605 and 1148 cm⁻¹, are seen. We assign the 2605 cm⁻¹ band to terminal a B–H stretch; terminal B–H stretches normally occur near 2600 cm⁻¹ in a wide variety of compounds.^{25–30} For comparison, an IR band at 2584 cm⁻¹ is assigned to the terminal B–H stretch of the Zr(BH₄)₄ precursor, which has four tridentate BH₄ groups, each of which bears one terminal hydrogen atom.

The 1148 cm⁻¹ feature seen for the ZrB_{2+x} film cannot be due to hydrogen atoms that bridge between boron and zirconium. Such bridging hydrogen atoms are signaled by bands at other frequencies: for example, in the Zr(BH₄)₄

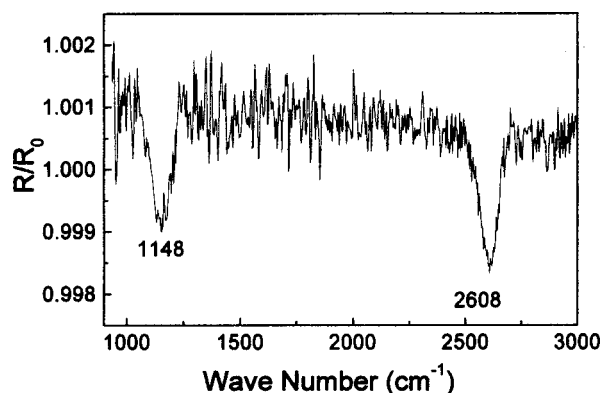


FIG. 2. Infrared reflectance spectrum of a SiO₂ surface (the optical cavity substrate) after exposure to Zr(BH₄)₄ at a partial pressure of 1.2×10^{-6} Torr for 67 s at 250 °C.

precursor the bridging hydrogen atoms give rise to IR bands at 2198 and 1223 cm⁻¹.^{24,31} Instead, we assign the 1148 cm⁻¹ band to a deformation mode of a BH₂ unit that bears two terminal hydrogen atoms: this deformation mode is typically seen between 1094 and 1175 cm⁻¹.^{25–30} We can rule out the possibility that the 1148 cm⁻¹ feature is due to the presence of oxidized species: the compounds B₂O₃, HBO₂, and B(OH)₃ do not have vibrational modes near 1150 cm⁻¹.^{32–34}

The bands at 2605 and 1148 cm⁻¹ seen for the ZrB_{2+x} film are therefore assigned to a terminal B–H stretch and a terminal BH₂ deformation mode, respectively. The presence of the latter mode rules out the possibility that intact Zr(BH₄)₄ molecules are present on the substrate. Instead, we believe that the excess boron in the as-deposited thermal-CVD films is largely (if not exclusively) present in the form of surface-bound BH₂ fragments, which are generated by incomplete reaction of the precursor. These BH₂ fragments oxidize readily in air, and the resulting formation of oxide phases significantly degrades the film properties.

B. Remote hydrogen plasma CVD

In an effort to deposit stoichiometric, single-phase ZrB₂ films, we added plasma-generated atomic hydrogen to the growth flux of Zr(BH₄)₄. We hypothesized that the atomic hydrogen would help to remove excess boron from the films by enhancing the formation and desorption of diborane.

The results are dramatic: films with B/Zr atomic ratios of 2 can be obtained at substrate temperatures of 300 °C (Fig. 3), provided that the flux of atomic hydrogen is sufficiently high (Fig. 4).³⁵ Such films have very low electrical resistivities (as low as 46 $\mu\Omega$ cm) and low oxygen contents (4 at. %) as discussed below. The use of atomic H also eliminates film blistering and oxidation after air exposure. The films grown by RPCVD at high temperatures have B/Zr ratios of less than 2; the substoichiometry is due to the residual incorporation of oxygen from the vacuum background during growth.

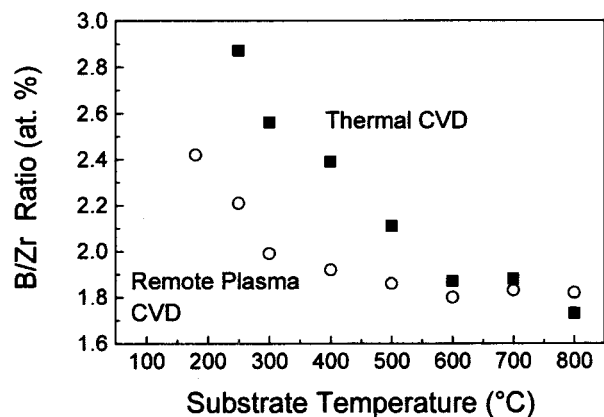


FIG. 3. B/Zr atomic ratio vs substrate temperature for thermal CVD (closed squares) and remote plasma CVD (open circles). The partial pressures of $Zr(BH_4)_4$ and H_2 were 1.2×10^{-5} and 2.3×10^{-3} Torr, respectively, and the plasma input power was 90 W.

In order to prove that the benefits of the remote plasma can be attributed to atomic rather than molecular hydrogen, we grew control samples by thermal CVD from mixtures of $Zr(BH_4)_4$ and H_2 . The films obtained are identical to those obtained from $Zr(BH_4)_4$ alone and suffer from the same problems: excess boron, blistering, and rapid oxidation in air.

1. Film purity

Carbon is not detectable in the RPCVD films by either RBS or XPS, and its concentration must therefore be less than 0.1 at. %. The principal impurity in the films is oxygen. Under RPCVD with a $Zr(BH_4)_4$ pressure of 1.2×10^{-5} Torr, a H_2 pressure of 2.3×10^{-3} Torr, a microwave plasma power of 90 W, and a substrate temperature of 250–400 °C, the oxygen concentration is <4 at. % and no further oxidation of the film occurs after air exposure. For ZrB_2 films prepared by a physical vapor deposition method, plasma-spraying, similar results have been reported: the oxygen content decreases when hydrogen is added to the argon carrier gas.³⁹ In contrast, films of ZrB_2 grown by thermal CVD from $Zr(BH_4)_4$ under otherwise identical conditions

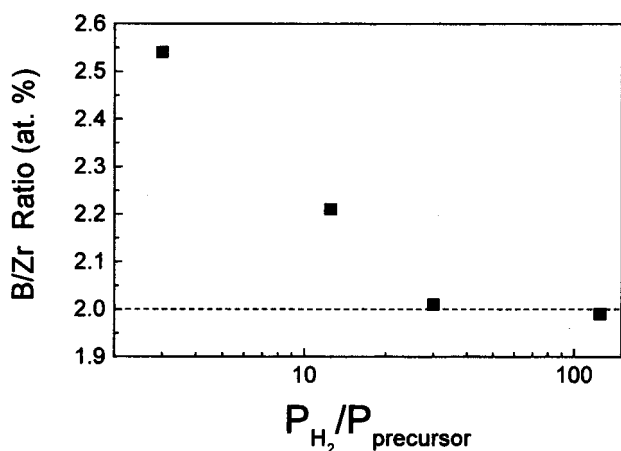


FIG. 4. B/Zr ratio of deposited films vs precursor partial pressure at $T_s = 300$ °C. The H_2 partial pressure was 2.3×10^{-3} Torr and the plasma input power was 90 W.

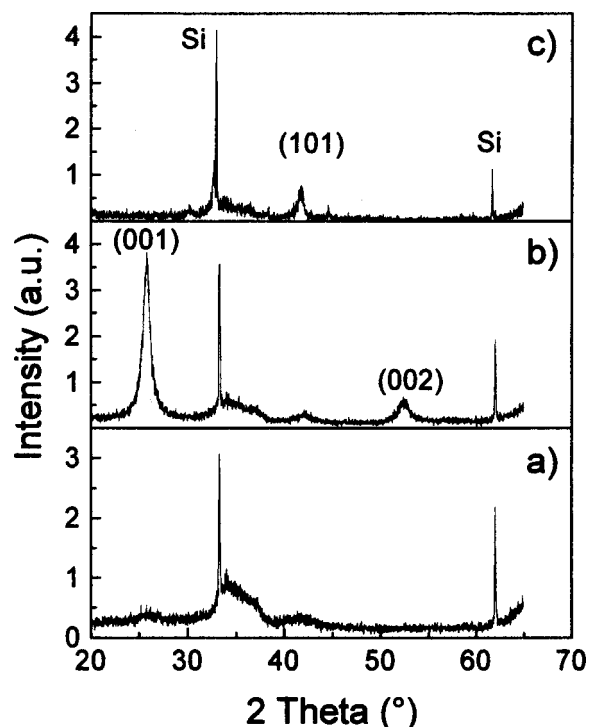


FIG. 5. X-ray diffraction profile of films grown (a) at $T_s = 300$ °C with a $Zr(BH_4)_4$ pressure of 1.2×10^{-5} Torr, (b) at $T_s = 500$ °C with a precursor pressure of 1.2×10^{-5} Torr, and (c) at $T_s = 500$ °C and a precursor pressure of 3.1×10^{-4} Torr. The H_2 partial pressure was 2.3×10^{-3} Torr and the plasma input power was 90 W.

contain 10–15 at. % oxygen; the concentration rises with an increase in substrate temperature and/or precursor pressure.

XPS data also reflect the reduction in oxygen content. In thermal CVD films, a large $Zr(3d^{5/2})$ peak at 183.5 eV indicates the presence of ZrO_2 ;³⁶ in RPCVD films grown with $T_s = 250$ – 300 °C and $Zr(BH_4)_4$ pressure $< 10^{-4}$ Torr, the 183.5 eV peak is nearly absent, as is the $B(1s)$ peak at 193 eV that would indicate the presence of boron oxide (B_2O_3).^{36–38} Owing to peak overlaps, the XPS data are not sufficient to determine the chemical environment of the oxygen remaining in the RPCVD films.

The presence of oxygen in the films has several possible explanations: (1) the $Zr(BH_4)_4$ precursor (which is air and water sensitive) contains a volatile oxygen-containing impurity that contributes to the film growth chemistry, (2) water present as a background gas (desorbed from the chamber wall or sample manipulator) reacts on the growth surface during deposition, or (3) postgrowth surface oxidation or hydrolysis occurs when the deposited films are handled in air. The first alternative is certainly possible; a likely candidate for a volatile oxygen-containing impurity is boric acid, $B(OH)_3$. In our experience, however, low oxygen contents are most clearly correlated with cleaner environments during deposition, which suggests that process (2) is important. Process (3) is eliminated by the finding that the oxygen content of the RPCVD films does not increase as the films are exposed to air for longer periods.

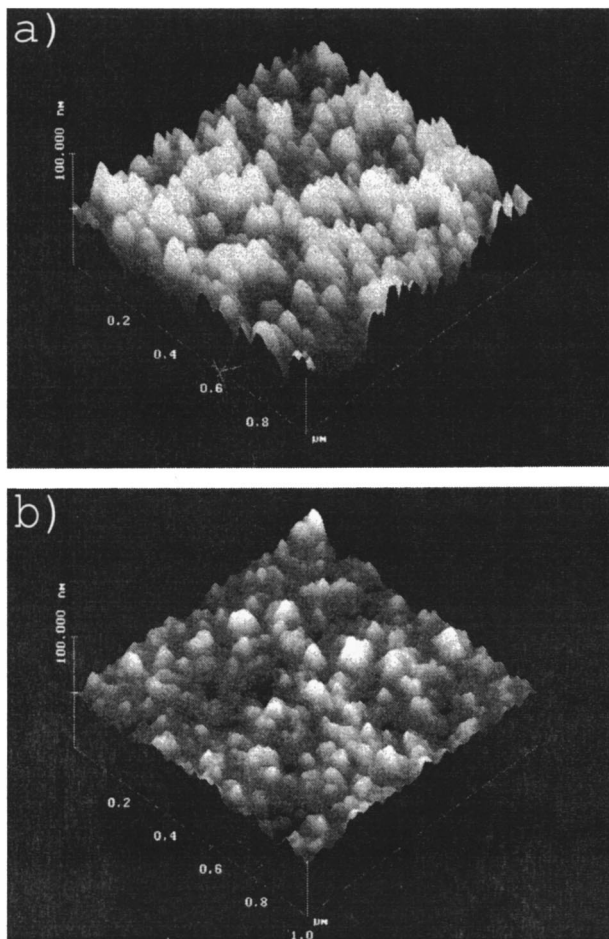


FIG. 6. AFM image of films grown at a substrate temperature of 300 °C by (a) thermal CVD (rms roughness=6.7 nm) and (b) remote hydrogen plasma CVD (rms roughness=4.3 nm).

2. Microstructure

XRD profiles show that the ZrB_2 films are crystalline if they are grown at substrate temperatures above 450 °C (Fig. 5). At lower temperatures, the films are amorphous. No diffraction peaks due to zirconium oxide or boron oxide are observed at any temperature.⁴⁰

The orientation of the crystallites relative to the substrate plane depends on the precursor partial pressure, which in turn controls the growth rate. At low growth rates (below 50 nm/min), there is a preference for the (001) basal plane of the hexagonal structure to be oriented parallel to the substrate plane; at faster growth rates, crystallites with the (101) plane parallel to the substrate plane are prevalent.

Atomic hydrogen dramatically reduces the surface roughness, as shown by AFM (Fig. 6). We suggest that an enhanced nucleation rate is the main reason for the smoother surface. Atomic hydrogen is known to enhance the nucleation of TiB_2 in hot wire CVD.⁴¹

3. Resistivity

Amorphous ZrB_{2+x} films deposited by thermal CVD exhibit high resistivities of $>300 \mu\Omega$ cm owing to the presence of excess boron and oxide impurities.¹⁶ In contrast, the films obtained by the RPCVD method exhibit resistivities as

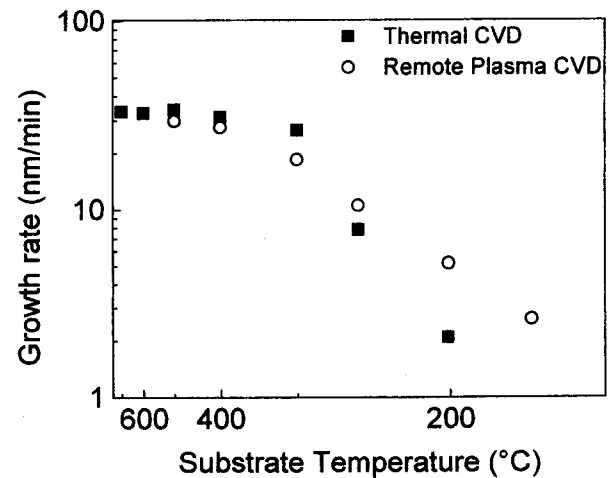


FIG. 7. Growth rate vs substrate temperature. The partial pressures of $Zr(BH_4)_4$ and H_2 were 1.2×10^{-5} and 2.3×10^{-3} Torr, respectively. The plasma input power was 90 W.

low as $46 \mu\Omega$ cm. For comparison, the resistivity of amorphous MOCVD TiN, which is widely used in current ULSI processing, is 250–350 $\mu\Omega$ cm.⁴² For the RPCVD ZrB_2 films, the lowest resistivities were obtained at the lower substrate temperatures; this finding reflects the fact that the oxygen content of the films is also minimized at lower temperatures, as described above.

4. Growth rate

The ZrB_2 growth rate with a $Zr(BH_4)_4$ partial pressure of 1.2×10^{-5} Torr was measured as a function of substrate temperature (Fig. 7). The behavior is typical of CVD: at low substrate temperatures ($T \leq 300$ °C) the growth is limited by the surface reaction rate, and at high substrate temperatures ($T > 300$ °C) the growth is limited by the precursor flux; when the precursor pressure is increased to 5.5×10^{-4} Torr, the growth rate at 500 °C increases from 30 to 500 nm/min (data point not shown). At temperatures below 300 °C, the growth rate is sensitive to whether or not the plasma is on. Under purely thermal CVD, growth occurs with an apparent activation energy of ~ 0.52 eV and the rate is < 1 nm/min at 180 °C; this finding is consistent with previous results.^{18,20} In the presence of the hydrogen plasma, growth occurs with an apparent activation energy of ~ 0.24 eV and the rate is ≥ 2 nm/min at 180 °C.

C. Diffusion barrier and step coverage properties

To test the ability of a RPCVD ZrB_2 film to serve as a diffusion barrier, a silicon substrate was first coated with a 20 nm film of amorphous ZrB_2 grown at 300 °C by RPCVD, and the resulting surface was then coated with 100 nm of PVD copper. When the heterostructure is heated, no changes are evident by XRD below 650 °C (Fig. 8). At 650 °C, the ZrB_2 film begins to crystallize. No XRD peaks due to copper silicide are evident even after the heterostructure is heated for 30 min at 700 °C. Only above 750 °C does Cu_3Si begin to form; no other phases could be detected by XRD. These results are consistent with the behavior of other amorphous

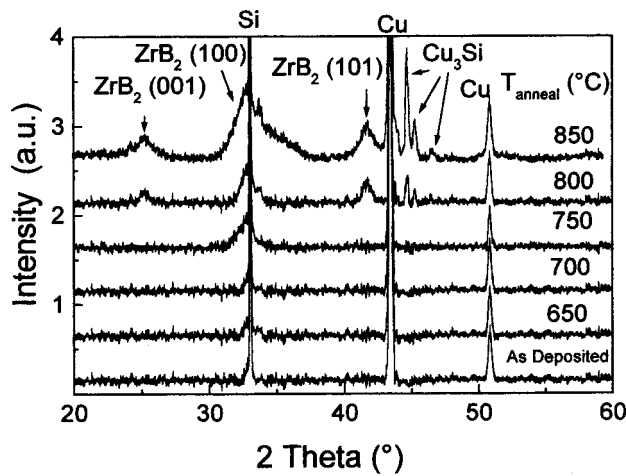


FIG. 8. X-ray diffraction profile of a Cu/ZrB₂/Si heterostructure after annealing at different temperatures for 30 min.

diffusion barriers, in which the main failure mechanism is crystallization of the barrier layer followed by diffusion through grain boundaries.⁴³

The conclusion that the RPCVD ZrB₂ films prevent diffusion up to 650 °C is supported by resistivity, RBS, and SEM data. The Cu sheet resistance (Fig. 9) is unaffected by heating the heterostructure to 650 °C. Above 750 °C, the sheet resistance begins to increase, a result that is consistent with the formation of copper silicide. RBS data (Fig. 10) also show that the Cu starts to diffuse through the ZrB₂ layer above 650 °C. Further information was obtained by annealing separate samples of Cu/ZrB₂/Si(100) heterostructures to successively higher temperatures, removing the copper layer and ZrB₂ barrier by etching in aqua regia, and then examining the silicon surface by SEM. For the samples annealed to temperatures of 650 °C or less, no pits or craters had formed on the surface of the Si substrate, and SIMS showed that no Cu was present in the Si.

In addition to the diffusion of Cu into Si, the diffusion of B into Si is also possible. If such a process occurs, the boron will serve as a *p*-type dopant and will significantly alter (in

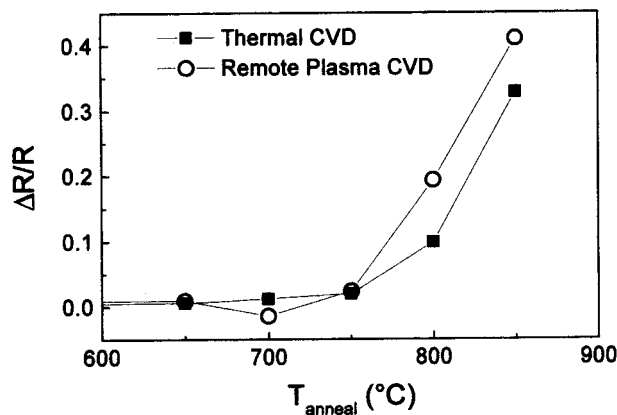


FIG. 9. Sheet resistance of a Cu/ZrB₂/Si heterostructure after annealing at different temperatures for 30 min.

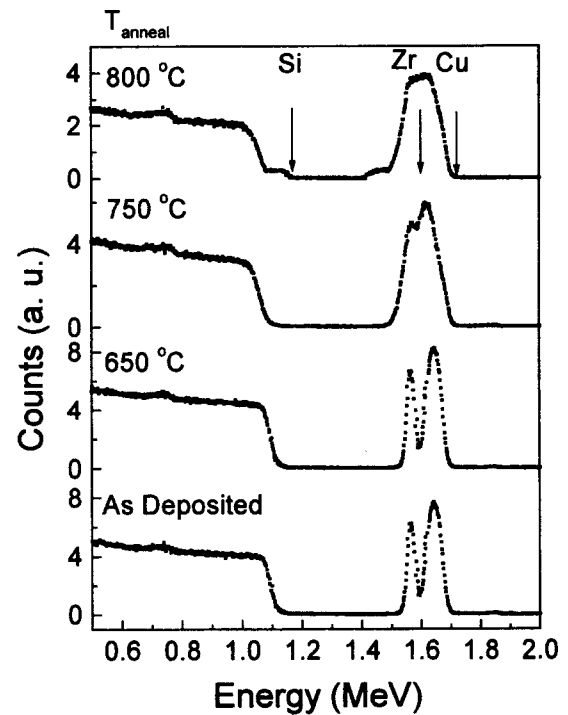


FIG. 10. RBS spectra of a Cu/ZrB₂/Si heterostructure after annealing at different temperatures for 30 min.

an undesirable way) the *I*–*V* properties of the Si substrate. To determine whether the extent of this B/Si diffusion process depends on the stoichiometry of the zirconium boride film, films were deposited by thermal CVD and by RPCVD on both *n*- and *p*-type Si substrates. The B/Zr ratio measured by RBS was 2.54 for the thermal CVD film and 1.96 for the RPCVD film. The *I*–*V* characteristics of the contact structures were measured at room temperature as a function of the annealing temperature. For the ZrB_{2+x} film grown by thermal CVD on *n*-type Si, a *p*-*n* junction starts to form upon annealing above 550 °C; by 650 °C the forward bias current is reduced to only 10⁻⁴ a at 2 V, not visible in the plot [Fig. 11(a)]. These changes presumably result from the diffusion of excess boron into the Si substrate. For the stoichiometric ZrB₂ film grown by RPCVD, the ohmic characteristics of the contact actually improve upon annealing to 500 °C, degrade slightly by 600 °C, and a *p*-*n* junction starts to form upon annealing to 650 °C. For thermal CVD films deposited on *p*-type Si, the diffusion of excess boron enhances the ohmic contact behavior after the sample is annealed to 750 °C; in contrast, annealing the RPCVD film yields only small changes. Thus we find evidence for significant diffusion of B from the thermal ZrB₂ film due to the presence of excess B, but a much smaller effect in the RPCVD film. These annealing temperatures are far above the limit of 400 °C for the “back end” processing of next-generation ULSI microelectronic devices.

The step-coverage characteristics of diffusion barriers are crucially important to the performance of ULSI devices. To test the ability of the RPCVD method to deposit conformal ZrB₂ films, a ~30 nm thick film was grown on top of a test wafer that featured a SiO₂ overlayer having 0.3 μm di-

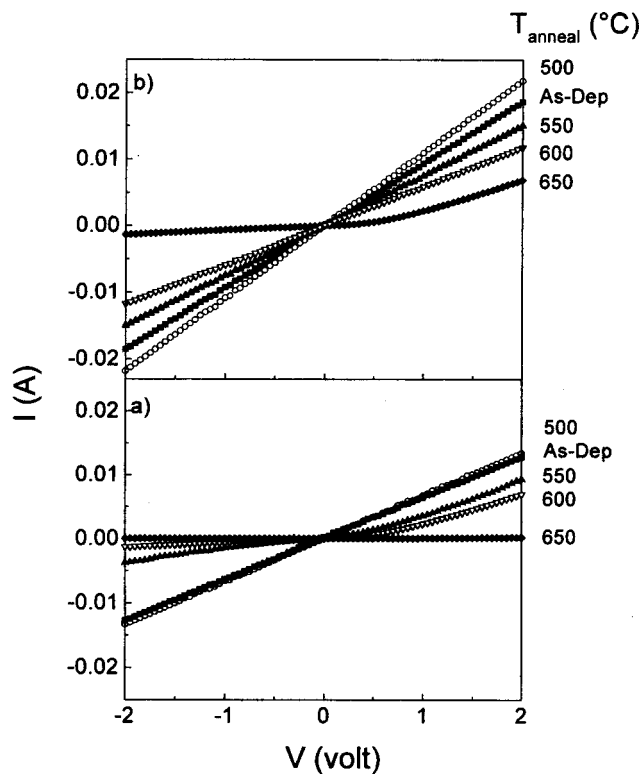


FIG. 11. I - V characteristics of ZrB_2 films deposited on n -type Si as a function of the annealing temperature. Films were grown by (a) thermal CVD ($B/Zr=2.54$) and (b) RPCVD ($B/Zr=1.96$).

ameter vias with 5:1 aspect ratios. SEM (Fig. 12) shows that the ZrB_2 film is highly conformal: the bottom coverage is $\sim 100\%$ that of the top layer and the sidewall coverage is $\sim 70\%$.

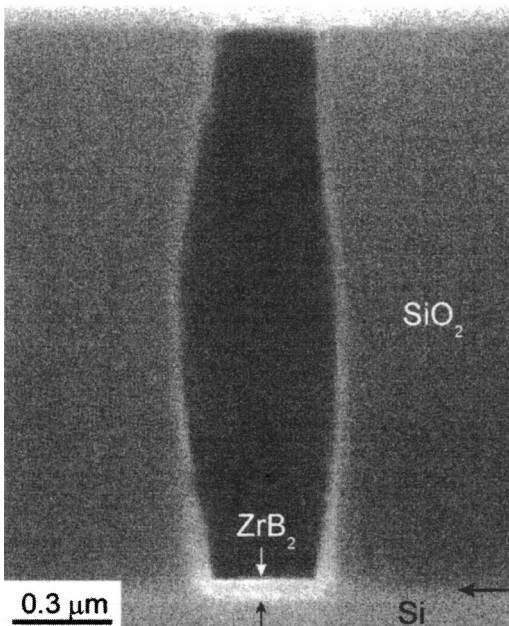


FIG. 12. SEM micrograph of a 30 nm thick ZrB_2 film deposited onto a 0.3 μm diameter via in SiO_2 by remote hydrogen plasma CVD at $T_s=300^\circ\text{C}$ with a $\text{Zr}(\text{BH}_4)_4$ pressure of 1.2×10^{-5} Torr and a H_2 pressure of 2.3×10^{-3} Torr. The plasma input power was 90 W.

IV. CONCLUSIONS

The problems previously reported for CVD growth of ZrB_2 films from $\text{Zr}(\text{BH}_4)_4$ -excess boron incorporation, severe oxygen contamination, and high electrical resistivity—are eliminated by simultaneously directing a flux of atomic hydrogen from a remote plasma source onto the growth surface. In thermal CVD (i.e., in the absence of the atomic hydrogen), the formation and release of diborane are inefficient relative to desorption of H_2 , and thus excess boron becomes trapped in the film, probably in the form of BH or BH_2 fragments. The thermal CVD films have B/Zr ratios near 3, have relatively high electrical resistivities, and oxidize readily in air. In contrast, by supplying atomic hydrogen during growth by RPCVD, diborane desorption is promoted and high-quality films are obtained even at low substrate temperatures. At 300°C , stoichiometric ZrB_2 films are obtained that have resistivities as low as $46 \mu\Omega \text{cm}$ and oxygen contents below $\sim 4 \text{ at. } \%$. These films are fully conformal in deep vias, and a 20 nm thick amorphous ZrB_2 film on c - $\text{Si}(001)$ prevents Cu indiffusion after 30 min annealing at 700°C . These properties suggest that RPCVD ZrB_2 films may be better Cu diffusion barriers than the metal nitride materials currently in use.

ACKNOWLEDGMENTS

The authors are grateful to the National Science Foundation for support of this research under Grant No. NSF CH00-76061. Compositional and structural analyses were carried out in the Center for Microanalysis of Materials, University of Illinois, which is supported by the U.S. Department of Energy under Grant No. DOE DEFG02-91ER45439. Electrical measurements were performed in the Microelectronics Laboratory at the University of Illinois.

¹K. Holloway and P. M. Fryer, Appl. Phys. Lett. **57**, 1736 (1990).

²P. Catania, J. P. Doyle, and J. J. Cuomo, J. Vac. Sci. Technol. A **10**, 3318 (1992).

³K. Chang, T. Yeh, I. Deng, and C. Shih, J. Appl. Phys. **82**, 1469 (1997).

⁴C. E. Ramberg, E. Blanquet, M. Pons, C. Bernard, and R. Madar, in Proceedings of the European Workshop Materials for Advanced Metallization, Oostende, Belgium, 1999.

⁵C. E. Ramberg, E. Blanquet, M. Pons, V. Ghetta, C. Bernard, and R. Madar, Mater. Res. Soc. Symp. Proc. **564**, 299 (1999).

⁶A. Jain, O. Adetutu, B. Ekstrom, G. Hamilton, M. Herrick, R. Venkatraman, and E. Weitzman, Mater. Res. Soc. Symp. Proc. **564**, 269 (1999).

⁷A. J. Becker and J. H. Blanks, Thin Solid Films **119**, 241 (1984).

⁸A. J. Caputo, W. J. Lackey, I. G. Wright, and P. Angelini, J. Electrochem. Soc. **132**, 2274 (1985).

⁹S. Motojima, M. Yamada, and K. Sugiyama, J. Nucl. Mater. **105**, 335 (1982).

¹⁰H. O. Pierson, E. Randich, and D. M. Mattox, J. Less-Common Met. **67**, 381 (1979).

¹¹A. Wang and G. Malé, J. Eur. Ceram. Soc. **11**, 241 (1993).

¹²H. O. Pierson and A. W. Mullendore, Thin Solid Films **95**, 99 (1982).

¹³S. Motojima, K. Sugiyama, and Y. Takahashi, J. Cryst. Growth **30**, 233 (1975).

¹⁴M. Hansen and K. Anderko, *Constitution of Binary Alloys* (McGraw-Hill, New York, 1958).

¹⁵S. Berthon, G. Pichelin, and G. Male, CALPHAD: Comput. Coupling Phase Diagrams Thermochem. **19**, 155 (1995).

¹⁶C. Y. Tay, I. R. Harris, and S. J. Wright, J. Electron. Mater. **16**, 107 (1987).

¹⁷T. Shikama, Y. Sakai, M. Fukutomi, and M. Okada, Thin Solid Films **156**, 287 (1988).

- ¹⁸J. A. Jensen, J. E. Gozum, D. M. Pollina, and G. S. Girolami, *J. Am. Chem. Soc.* **110**, 1643 (1988).
- ¹⁹H. R. Hoekstra and J. J. Katz, *J. Am. Chem. Soc.* **71**, 2488 (1949).
- ²⁰A. L. Wayda, L. F. Schneemeyer, and R. L. Opila, *Appl. Phys. Lett.* **53**, 361 (1988).
- ²¹W. E. Reid, J. M. Bish, and A. Brenner, *J. Electrochem. Soc.* **104**, 21 (1957).
- ²²M. Katiyar, Y. H. Yang, and J. R. Abelson, *J. Appl. Phys.* **77**, 6247 (1995).
- ²³www.genplot.com.
- ²⁴P. H. Bird and M. G. H. Wallbridge, *J. Chem. Soc., Chem. Commun.* 687 (1968).
- ²⁵W. C. Price, H. C. Longuet-Higgins, B. Rice, and T. F. Young, *J. Chem. Phys.* **17**, 217 (1949).
- ²⁶W. C. Price, *J. Chem. Phys.* **15**, 614 (1947).
- ²⁷W. C. Price, *J. Chem. Phys.* **16**, 894 (1948).
- ²⁸W. C. Price, *J. Chem. Phys.* **17**, 1044 (1949).
- ²⁹J. W. Nibler and J. McNabb, *J. Chem. Soc., Chem. Commun.* 134 (1969).
- ³⁰A. R. Emery and R. C. Taylor, *Spectrochim. Acta* **16**, 1455 (1960).
- ³¹T. J. Marks, W. J. Kennelly, J. R. Kolb, and L. A. Shimp, *Inorg. Chem.* **11**, 2540 (1972).
- ³²W. Welmer and J. R. W. Warn, *J. Chem. Phys.* **37**, 292 (1962).
- ³³S. K. Gupta and R. F. Porter, *J. Phys. Chem.* **67**, 1286 (1963).
- ³⁴B. S. Ault, *Chem. Phys. Lett.* **157**, 547 (1989).
- ³⁵If our microwave plasma source could generate additional atomic H, then the RPCVD curve shown in Fig. 3 presumably would shift to even lower temperatures.
- ³⁶NIST on-line XPS database: <http://srdata.nist.gov/xps/>
- ³⁷M. Belyansky and M. Trenary, *J. Vac. Sci. Technol. A* **15**, 3065 (1997).
- ³⁸M. Belyansky and M. Trenary, *Chem. Mater.* **9**, 403 (1997).
- ³⁹P. V. Ananthapadmanabhan, K. P. Sreekumar, P. V. Ravindran, and N. Venkatramani, *Thin Solid Films* **224**, 148 (1993).
- ⁴⁰J. F. Pierson, A. Billard, T. Belmonte, H. Michel, and C. Frantz, *Thin Solid Films* **347**, 78 (1999).
- ⁴¹J. Elders and J. D. W. van Voorst, *Appl. Surf. Sci.* **69**, 267 (1993).
- ⁴²S. R. Kurtz and R. G. Gordon, *Thin Solid Films* **140**, 277 (1986).
- ⁴³G. S. Chen, P. Y. Lee, and S. T. Chen, *Thin Solid Films* **353**, 264 (1999).

Journal of Applied Physics is copyrighted by the American Institute of Physics (AIP). Redistribution of journal material is subject to the AIP online journal license and/or AIP copyright. For more information, see <http://ojps.aip.org/japof/japocr/jsp>
Copyright of Journal of Applied Physics is the property of American Institute of Physics and its content may not be copied or emailed to multiple sites or posted to a listserv without the copyright holder's express written permission. However, users may print, download, or email articles for individual use.